

## Effects of cations on rare earth adsorption and desorption in binding sites of montmorillonite

Zhengyan He <sup>1</sup>, Wenrui Nie <sup>1</sup>, Huifang Yang <sup>1, 2</sup>, Yuchen Tang <sup>1</sup>, Aoyang Sha <sup>1</sup>, Jun Qu <sup>1</sup>, Zhigao Xu <sup>1</sup>, Ruan Chi <sup>2</sup>

<sup>1</sup> Key Laboratory of Resources Conversion and Pollution Control of the State Ethnic Affairs Commission, College of Resources and Environmental Science, South-Central Minzu University, Wuhan 430074, Hubei, PR China

<sup>2</sup> Key Laboratory for Green Chemical Process of Ministry of Education, School of Resources & Safety Engineering, Wuhan Institute of Technology, Wuhan 430073, Hubei, PR China

Corresponding author: xuzhigaotc@126.com (Zhigao Xu)

**Abstract:** The exchangeability of rare earth (RE) in weathered crust elution-deposited rare earth ores largely depends on its interaction with clay minerals, which may be significantly influenced by various cations. Therefore, the effects of  $K^+$ ,  $Ca^{2+}$  and  $Al^{3+}$  on  $RE^{3+}$  adsorption and desorption in binding sites of montmorillonite (MMT) were investigated. Through the pre-saturation, the interlayer ions of MMT had been replaced by  $K^+$ ,  $Ca^{2+}$  or  $Al^{3+}$ .  $RE^{3+}$  can adsorb on the interlayer sites of Ca-MMT and K-MMT, but nearly not Al-MMT. The basal spacing of Ca-MMT is larger than K-MMT, which provides a smaller hinder effect of interlayer collapse for the interlayer diffusion of  $RE^{3+}$ . The adsorption capacity followed the order: Ca-MMT > K-MMT > Al-MMT and  $La^{3+} > Y^{3+} > Eu^{3+}$ . It can predict that the grade of the exchangeable RE in ores abundant in  $Ca^{2+}$  is the most, followed by the ore rich in  $K^+$  and  $Al^{3+}$  the least. Clay minerals tend to adsorb light RE and hard to adsorb middle and heavy RE. The reversibility of RE adsorbed in interlayers, especially in collapsed interlayers, is far worse than that on externals. The desorption rates of RE were in the order of RE-Al-MMT > RE-K-MMT > RE-Ca-MMT and  $Eu^{3+} > Y^{3+} > La^{3+}$ . For the desorption of interlayer  $RE^{3+}$ ,  $NH_4^+$  is better than  $Mg^{2+}$  because the larger change of the basal spacings ( $\Delta d$ ) provides more minor activation energy barriers ( $\Delta E$ ) for  $NH_4^+$  diffusion within interlayers. It can enrich the metallogeny theory of weathered crust elution-deposited rare earth ores and provide a certain theoretical basis for its efficient exploitation.

**Keywords:** adsorption, desorption, external site, interlayer site, basal spacing, weathered crust elution-deposited rare earth ores

### 1. Introduction

Rare earth (RE) elements have unique physical properties such as magnetic, optical, electrical, etc. It is often called "the treasury of new material in the 21<sup>st</sup> century" and "industrial vitamins", and is widely applied in high-tech and national defense fields, like magnetism, luminescence, laser, optical fiber, hydrogen storage, superconductivity, et al (Chen et al., 2011; Kanazawa and Kamitani, 2006). According to the differences in their sulfate solubility, rare earths can be classified into light rare earths (La, Ce, Pr and Nd), middle rare earths (Sm, Eu, Gd, Tb and Dy) and heavy rare earths (Ho, Er, Tm, Yb, Lu and Y), in which the middle and heavy rare earths with a higher application and commercial value only account for about 10%. Weathered crust elution-deposited rare earth ores (WCE-DREO) play a vital role in the international market because it is rich in 80% of middle and heavy rare earths in the world's total reserves (Chi and Tian, 2008).

Under the chemical, physical and biological effects, protoliths including RE (e.g. volcanic, granite, et al.) are weathered to form clay minerals (e.g. halloysite, kaolinite and montmorillonite, et al.). Simultaneously, RE minerals (e.g. gadolinite, bastnaesite, aeschynite, et al.) in protoliths are also weathered and dissociated to hydrated RE ions or hydroxyl hydrated RE ions, which adsorb on the

above clay minerals. This is the metallogeny of WCE-DREO (Chi and Wang, 2014). Consequently, 60~90% of RE in WCE-DREO exists in the form of an ionic phase, which can be recovered by ion-exchange method using electrolyte solution (Chi et al., 2005; Tian et al., 2013).

Due to a high leaching efficiency of RE, ammonium salt as a leaching agent is widely applied in the recovery of RE from WCE-DREO. Nevertheless, ammonium salt may cause a certain ammonia nitrogen pollution to the environment, especially the water body (Huang et al., 2021; Feng et al., 2021). To solve this problem, many non-ammonium leaching agents have been proposed, such as magnesium sulfate (Xiao et al., 2015a; 2015b), ferrous sulfate (Xiao et al., 2016a; 2017), aluminum sulfate (Yang et al., 2019), etc. Among them, magnesium sulfate is the most promising and has been used in some WCE-DREO, although its leaching capacity for RE is slightly lower than ammonium sulfate (Xiao et al., 2015a). The leaching capacity of leaching agents for RE is varied with the exchangeability between cations in the leaching agents with RE ions. Generally, cations with a small hydration radius or low hydration energy may have a strong exchangeability and can easily desorb RE ions from WCE-DREO (Moldoveanu and Papangelakis, 2012).

The leaching efficiency of RE is not only related to leaching agents, but also to the composition of the binding site of RE adsorbed on clay minerals (Fan et al., 2014). In general, the binding sites of metal cations on clay minerals can be simply divided into external sites with low affinity and interlayer sites with high affinity (Yin et al., 2017). RE adsorbed on external sites may be readily replaced by other cations, while RE intercalated into interlayer sites may be exchanged only by particular cations, and the difficulty of RE exchangeability increases from edge to center along with the interlayers (Rigol et al., 1999). The exchangeability of RE adsorbed on external sites is far better than the one on interlayer sites, especially the center sites of the interlayer. Hence, the more RE adsorbed on interlayer sites, the lower the leaching efficiency of RE is.

The characteristic of the interlayer sites can be altered by interlayer changes that further affects the adsorption of RE on the interlayer. In the formation process of WCE-DREO, various cations (e.g.  $K^+$ ,  $Ca^{2+}$  and  $Al^{3+}$ , et al.) are released into soils due to the partial dissociation of minerals and the decomposition of organic matters (Li, 2014). These released cations will migrate down the orebody with the rainwater, meanwhile enter the interlayer of clay minerals and exchange with the interlayer cations which result in the collapse or expansion of interlayers (Rigol et al., 1999). The change of interlayer spacing will alter the adsorption characteristic of the interlayer for RE, which further affects the exchangeability of interlayer RE (Dzene et al., 2017). The species and content of cations in soils located in various ore areas must be different, which leads to the different composition of the binding site of RE adsorbed on clay minerals (Benedicto et al., 2014). Hence, the leaching efficiency of RE from diverse WCE-DREO may be different, even if using the same leaching agent and under the same leaching conditions. Xiao et al. (2015c) investigated the leaching process of WCE-DREO located in Longnan and Liutang, and found that the leaching efficiency of RE from Longnan RE ores was always lower than the one from Liutang RE ores under the same conditions. It can be observed that the cations will affect the RE adsorption and desorption in different binding sites of clay minerals. However, little attention has been paid to it at present. Most researchers studied the adsorption capacity of RE on the clay minerals at a macro-level, and then applied adsorption models to predict the adsorption styles of RE on the clay minerals at a micro-level (Alshameri et al., 2019; Coppin et al., 2002; Sinitsyn et al., 2000; Wan and Liu, 2006; Xiao et al., 2016b; Yang et al., 2019; Yu et al., 2019; Zhou et al., 2019).

The main purpose of this study is to clarify the effect of cations ( $K^+$ ,  $Ca^{2+}$  and  $Al^{3+}$ ) on the interlayer structure of clay minerals and how this affects the adsorption and desorption of RE in different binding sites of clay minerals. The adsorption ability of montmorillonite (MMT) to RE is best among clay minerals, so MMT was selected as the research object. The original MMT was initially treated by saturation with  $K^+$ ,  $Ca^{2+}$  or  $Al^{3+}$  solution. The adsorption of La, Eu and Y on treated MMT was investigated, and its extractability was subsequently evaluated with  $NH_4Cl$ ,  $(NH_4)_2SO_4$ ,  $MgCl_2$  and  $MgSO_4$ . The study of La, Eu and Y is beneficial to reveal the migration and enrichment regularity of light, middle and heavy RE in WCE-DREO. Ammonium salts ( $(NH_4)_2SO_4$  and  $NH_4Cl$ ) and magnesium salts ( $MgSO_4$  and  $MgCl_2$ ) were all selected as the desorption agent to compare the leaching mechanism and leaching capacity of the traditional and novel leaching agents. The results can guide the

development of high-efficiency leaching agents and the selection of leaching agents in practice. It can also enrich the metallogeny theory of WCE-DREO and provide a certain theoretical basis for the efficient exploitation of WCE-DREO.

## 2. Materials and methods

### 2.1. Materials

MMT purchased from Huadu in Guangzhou, China was ground and sieved, and the samples with a particle size of 50-150  $\mu\text{m}$  were dried in an oven at 60°C for later use. The mineral composition of MMT was analyzed by X-ray diffraction (XRD, MAX-RB RU-200B, Rigaku Corporation, Japan). The purity of MMT is more than 80% containing a small amount of kaolinite and  $\text{CaCO}_3$ .

$\text{LaCl}_3 \cdot 7\text{H}_2\text{O}$ ,  $\text{EuCl}_3 \cdot 6\text{H}_2\text{O}$  and  $\text{YCl}_3 \cdot 6\text{H}_2\text{O}$  with a purity of 99.9% were purchased from Shanghai Aladdin Biochemical Technology Co., Ltd.  $\text{KCl}$ ,  $\text{CaCl}_2$ ,  $\text{NH}_4\text{Cl}$ ,  $\text{MgCl}_2$  and  $(\text{NH}_4)_2\text{SO}_4$  were of analytical grade and bought from Shanghai Sinopharm Chemical Reagent Co., Ltd.  $\text{AlCl}_3 \cdot 6\text{H}_2\text{O}$  and  $\text{MgSO}_4 \cdot 7\text{H}_2\text{O}$  were purchased from Shanghai Lingfeng Chemical Reagent Co., Ltd. All the reagents employed in this study were used as received without further purification.

### 2.2. Pretreatments of MMT

In order to better know the adsorption behaviors of RE on MMT, the homogeneous samples with single ion morphology were prepared as the following method. 10 g of MMT with a particle size of 50-150  $\mu\text{m}$  was added into 100 mL 0.5 mol  $\cdot\text{L}^{-1}$   $\text{KCl}$ ,  $\text{CaCl}_2$  or  $\text{AlCl}_3$  solutions. The mixed solution was oscillated in a thermostatic oscillator at 25°C and 180 rpm for two days. After the solid-liquid separation, the separated solids were repeated the above treatment twice to reach saturated adsorption. The final solids were rinsed with deionized water to remove the excess cations, then dried at 60°C for 24 h. The  $\text{K}^+$ ,  $\text{Ca}^{2+}$  and  $\text{Al}^{3+}$  pretreated MMTs can simply express as K-MMT, Ca-MMT and Al-MMT, respectively, which were used for the characterization analysis and RE adsorption experiments.

### 2.3. RE adsorption on pretreated MMT

1.0 g pretreated MMT was added into 100 mL 1000 ppm  $\text{LaCl}_3$ ,  $\text{EuCl}_3$  and  $\text{YCl}_3$  solutions, respectively. In order to achieve the adsorption equilibrium, the mixed solution oscillated in a thermostatic oscillator at 30°C and 180 rpm for one week. After standing 6 h, the supernatant was filtered through a 0.22  $\mu\text{m}$  membrane to determine RE concentration using an Inductively coupled plasma emission spectrometer (ICP-OES, Avio200, Perkin Elmer Inc., USA). The solids adsorbed RE were dried at 60°C for 24 h before the characterization analysis. K-MMT adsorbed  $\text{La}^{3+}$ ,  $\text{Eu}^{3+}$  and  $\text{Y}^{3+}$  can be abbreviated to La-K-MMT, Eu-K-MMT, Y-K-MMT, respectively. The abbreviated forms of Ca-MMT and Al-MMT adsorbed  $\text{La}^{3+}$ ,  $\text{Eu}^{3+}$  and  $\text{Y}^{3+}$  are the same as the K-MMT adsorbed RE.

### 2.4. RE desorption experiments

The RE desorption experiments were performed according to a well-established semicontinuous batch approach (Rigol et al., 1999) composed of four desorption cycles. 0.1000 g RE-K/Ca/Al-MMT was added into 10 mL  $\text{NH}_4\text{Cl}$ ,  $\text{MgCl}_2$ ,  $(\text{NH}_4)_2\text{SO}_4$  and  $\text{MgSO}_4$  solutions with a cation concentration of 0.2 mol  $\cdot\text{L}^{-1}$ , respectively. The mixed solution oscillated in a thermostatic oscillator at 30°C and 180 rpm. The desorption time was one day for the first three cycles and five days for the fourth cycle. After every desorption cycle, the separated solid sample without drying was directly dispersed into the same freshly prepared solution, and the supernatant was filtered through a 0.22  $\mu\text{m}$  membrane for the analysis of RE concentration by ICP-OES. According to the RE concentration before and after desorption, the desorption ratio of each cycle can be calculated. To ensure the accuracy of the data, each desorption experiment was repeated at least three times. The whole experiment processes are shown in Fig.1.

### 2.5. XRD analysis

Once the ion exchange occurs in the interlayer of clay minerals, the interlayer spacing will change due

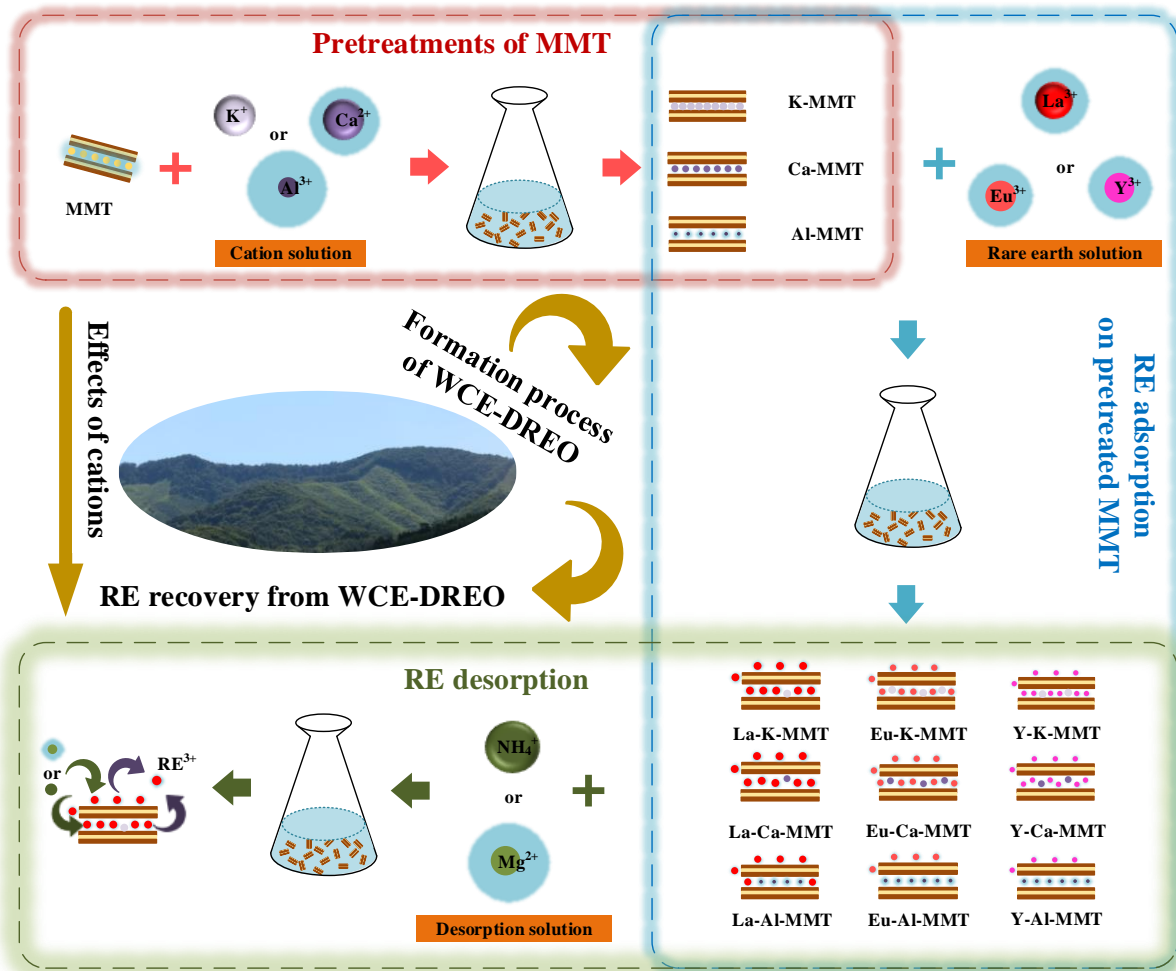


Fig. 1. Schematic diagram of whole experimental processes

to the different ion radius. The change can cause the shift of the diffraction peak for 001 reflections, which can be observed by XRD (Dzene et al., 2015; Tombacz and Szekeres, 2004). To investigate the cation exchange on MMT in the whole experimental processes, the pretreated, RE saturated and desorbed MMT specimens were analyzed by XRD with  $2\theta$  angle scanning from  $4^\circ$  to  $10^\circ$  at a step-interval angle of  $0.02^\circ$ . The generator settings were at a current of 40 mA and a voltage of 40 kV with a Cu-K $\alpha$  ( $\lambda = 0.154$  nm) radiation. According to the results of XRD, the basal spacing ( $d_{001}$ ) of MMT can be calculated by Bragg's equation (Lee et al., 2017; Tertre 2011; Pope, 1997).

$$2d\sin\theta = n\lambda \quad (1)$$

where  $\lambda$  is the wavelength of XRD used,  $d$  is the spacing between diffraction lattice planes,  $\theta$  is the measured diffraction angle, and  $n = 1, 2$ .

### 3. Results and discussion

#### 3.1. Interlayer change of MMT after pretreatment

The ionic radius, hydrated radius and hydration energy of related cations in this study are illustrated in Table 1 (Tansel et al., 2006; Tansel, 2012). When ions with a low (i.e.,  $K^+$ ) or high (i.e.,  $Ca^{2+}$  and  $Al^{3+}$ ) hydration energy enter the interlayer of MMT and reach saturation, the basal spacing ( $d_{001}$ ) of MMT will alter according to the different properties of ions. Thus, the cation exchange process involved in interlayer sites can be characterized by XRD. The XRD results of the untreated and pretreated MMT are presented on the left of Fig. 2. The characteristic peak of untreated MMT is at  $5.1^\circ$ , corresponding to the basal spacings of 17.25 Å. After being pre-saturated with  $K^+$ ,  $Ca^{2+}$  or  $Al^{3+}$ , the characteristic peak of MMT moves to  $6.7^\circ$ ,  $5.7^\circ$  and  $5.1^\circ$ , respectively, and the basal spacings are 13.22 Å, 15.74 Å and

17.31 Å, respectively. It indicates that after pretreatment, the characteristic diffraction peaks of MMT have evidently moved and varied with the pre-saturated cations. There must be an ion exchange in the interlayer of MMT, resulting in the change of the basal spacings in the pretreatment process. The basal spacings increase with the order of K-MMT, Ca-MMT and Al-MMT, which corresponds to their hydrated radius.

Table 1. Ionic radius, hydrated radius and hydration energy of cations

Cations	K <sup>+</sup>	Ca <sup>2+</sup>	Al <sup>3+</sup>	NH <sub>4</sub> <sup>+</sup>	Mg <sup>2+</sup>	La <sup>3+</sup>	Eu <sup>3+</sup>	Y <sup>3+</sup>
Ionic radius (Å)	1.33	1.01	0.53	1.48	0.72	1.03	0.95	0.89
Hydrated radius (Å)	3.31	4.12	4.80	3.31	4.28	—	—	—
Hydration energy (kJ/mol)	321	1557	4665	322	1828	3285	3508	—

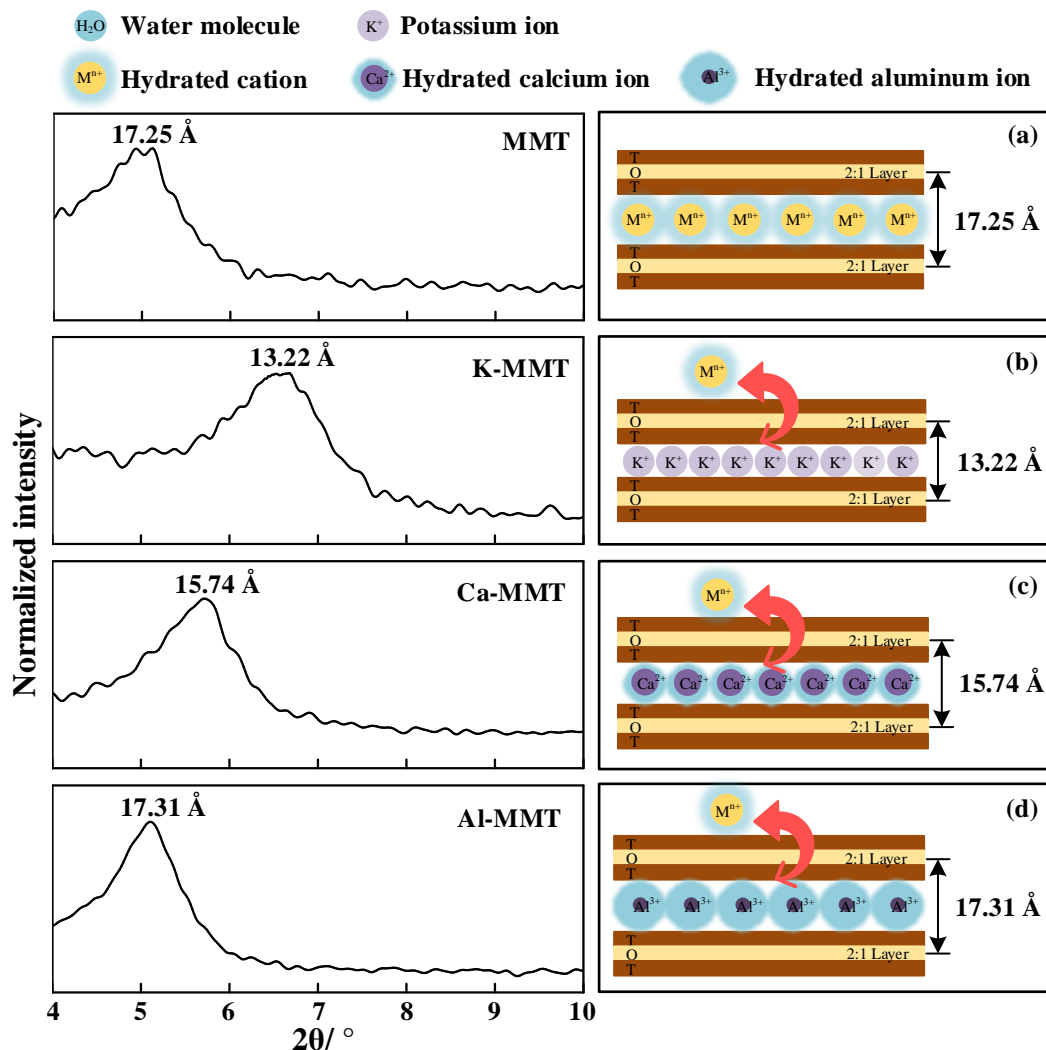


Fig. 2. XRD patterns (left) and assumed interlayer schematic diagram (right) of the untreated MMT (a) and pretreated MMT by saturation with K<sup>+</sup> (b), Ca<sup>2+</sup> (c) or Al<sup>3+</sup> (d)

The assumed interlayer schematic diagram of untreated and pretreated MMT is shown on the right of Fig. 2. The basal spacing of the untreated MMT (17.25 Å) is far larger than anhydrous Na-MMT (~9.6 Å) (Zhao and Zhang, 1990; Krishna and Susmita, 2009). So, the interlayer of the untreated MMT in this study must contain a certain number of ions and water molecules (shown in Fig. 2(a)). When MMT was placed in a high concentration of K<sup>+</sup>, Ca<sup>2+</sup> or Al<sup>3+</sup> solution, the cations in the solution can exchange the cations on the MMT and adsorb on the external (planar/edge sites) and interlayer sites of MMT. The cation exchange in interlayer sites must cause the change of the basal spacings. K<sup>+</sup> with a

small ionic radius (1.33 Å) and low hydration energy (321 kJ/mol) enter the interlayer of MMT in an anhydrous state and exchange the interlayer cations, resulting in the interlayer collapse. The basal spacing decreases from 17.25 Å to 13.22 Å (shown in Fig. 2(b)). Ca<sup>2+</sup> and Al<sup>3+</sup> with high hydration energy enter the interlayer of MMT in a hydration state, replace the interlayer cations and extrude the interlayer water, which causes the change of the basal spacings. Due to the different hydrated radius of Ca<sup>2+</sup> and Al<sup>3+</sup>, the interlayer of MMT collapses and the basal spacing decreases to 15.74 Å in Ca<sup>2+</sup> solution (shown in Fig. 2(c)), while the interlayer of MMT swells in Al<sup>3+</sup> solution and the basal spacing increases to 17.31 Å (shown in Fig. 2(d)). As a result, the structural transformations of MMT from the original ions interlayer to K<sup>+</sup>, Ca<sup>2+</sup> and Al<sup>3+</sup> replaced interlayers are achieved through the pretreatment with K<sup>+</sup>, Ca<sup>2+</sup> or Al<sup>3+</sup> solution.

### 3.2. Effect of interlayer change on RE adsorption on pretreated MMT

To understand the ions exchange properties of RE with the known characteristics of MMT and the effect of interlayer change on the distribution of RE adsorption sites, the RE adsorption behaviors on the three pretreated MMT were investigated. The saturated adsorption amounts of RE on the pretreated MMT were listed in Table 2. For the same rare earth element (REE), the adsorption capacity of the pretreated MMT decreases with the order of Ca-MMT, K-MMT and Al-MMT. Compared to K-MMT, Ca-MMT can provide more ion exchange sites due to a strong adsorption capacity of Ca<sup>2+</sup> on MMT and exchange more RE<sup>3+</sup> under a same number of ion exchange sites due to a high valence state of Ca<sup>2+</sup>. MMT pre-saturated with Al<sup>3+</sup> is acidic, which is not conducive to the adsorption of RE<sup>3+</sup> (Chi and Wang, 2014). Consequently, the adsorption capacity of Ca-MMT on RE is the strongest and Al-MMT is the weakest in the studied pre-treated MMT. For a same pretreated MMT, the adsorption capacity of RE increases with the order of Eu<sup>3+</sup>, Y<sup>3+</sup> and La<sup>3+</sup>. It indicates that the pre-treated MMT tends to adsorb light REE and hard to adsorb middle REE.

Table 2. Saturated adsorption amounts of RE on pretreated MMT (mmol/g)

Pretreated MMT	La <sup>3+</sup>	Eu <sup>3+</sup>	Y <sup>3+</sup>
K-MMT	0.30	0.25	0.28
Ca-MMT	0.37	0.26	0.30
Al-MMT	0.21	0.19	0.21

In aqueous solution, RE<sup>3+</sup> exists in the form of hydrated ions due to a high hydration energy. The hydrated radius of RE<sup>3+</sup> is larger than K<sup>+</sup> and Ca<sup>2+</sup>, but smaller than Al<sup>3+</sup> (Marcus, 1985). If the hydrous RE<sup>3+</sup> enters the interlayer of pre-treated MMT, the basal spacing of K-MMT and Ca-MMT will increase due to the interlayer swelling and the basal spacing of Al-MMT will decrease due to the interlayer collapse. The more RE ions enter the interlayer, the greater the change in the basal spacing (Yin et al., 2017). The XRD patterns of K-MMT, Ca-MMT and Al-MMT before and after RE adsorption are compared in Fig. 3 to 5. The characteristic diffraction peak of Al-MMT shifts slightly to the right after La<sup>3+</sup> saturation and is nearly unchanged after Eu<sup>3+</sup> and Y<sup>3+</sup> saturation. It indicates that only a small La<sup>3+</sup> can enter the interlayer of Al-MMT to exchange Al<sup>3+</sup>, and Eu<sup>3+</sup> and Y<sup>3+</sup> cannot. Most of the adsorbed RE<sup>3+</sup> can be confidently ascribed to its binding on the external sites of Al-MMT rather than the interlayer sites. Considering the adsorption capacity listed in Table 2, it can conjecture preliminarily that the adsorption amount of RE<sup>3+</sup> on the external sites of Al-MMT follows the order: La<sup>3+</sup> (0.21 mmol/g)  $\approx$  Y<sup>3+</sup> (0.21 mmol/g) > Eu<sup>3+</sup> (0.19 mmol/g).

Unlike Al-MMT, the characteristic diffraction peaks of K-MMT and Ca-MMT obviously move to the left after adsorbed RE<sup>3+</sup>, implying an increase in the basal spacings. There must be an ion exchange between RE<sup>3+</sup> and K<sup>+</sup>/Ca<sup>2+</sup> in the interlayer of K-MMT and Ca-MMT. RE<sup>3+</sup> can not only adsorb on the external sites of K-MMT and Ca-MMT, but also adsorb on the interlayer sites. Thus, the adsorption capacity of RE<sup>3+</sup> on K-MMT and Ca-MMT is both stronger than Al-MMT. After adsorbed La<sup>3+</sup>, Eu<sup>3+</sup> or Y<sup>3+</sup>, the basal spacing of Ca-MMT is 17.64 Å, 17.32 Å and 17.58 Å, respectively, which are all larger than K-MMT (17.38 Å for La<sup>3+</sup>, 17.10 Å for Eu<sup>3+</sup> and 14.97 Å for Y<sup>3+</sup>). Compared to K-MMT, there must be more RE<sup>3+</sup> entering the interlayer of Ca-MMT, resulting in a larger adsorption capacity of RE<sup>3+</sup> on

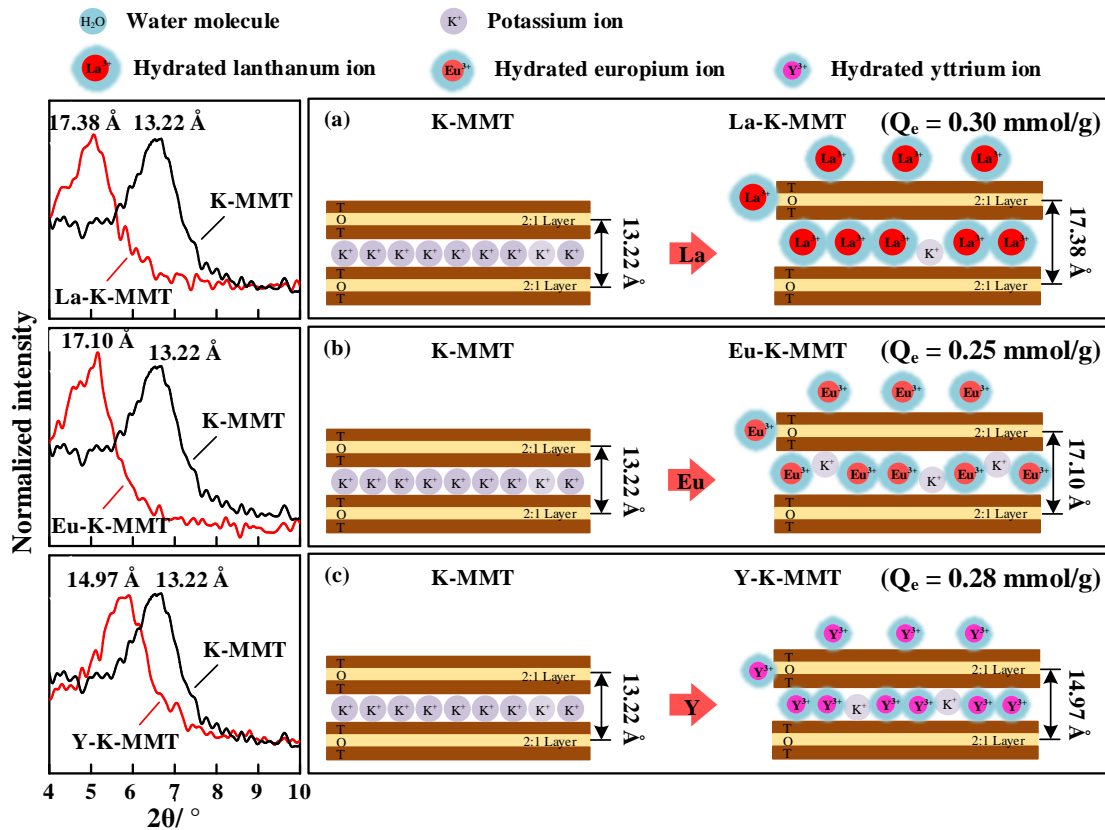


Fig. 3. XRD patterns (left) and assumed schematic diagrams (right) of K-MMT before and after La<sup>3+</sup> (a), Eu<sup>3+</sup> (b) or Y<sup>3+</sup> (c) adsorption

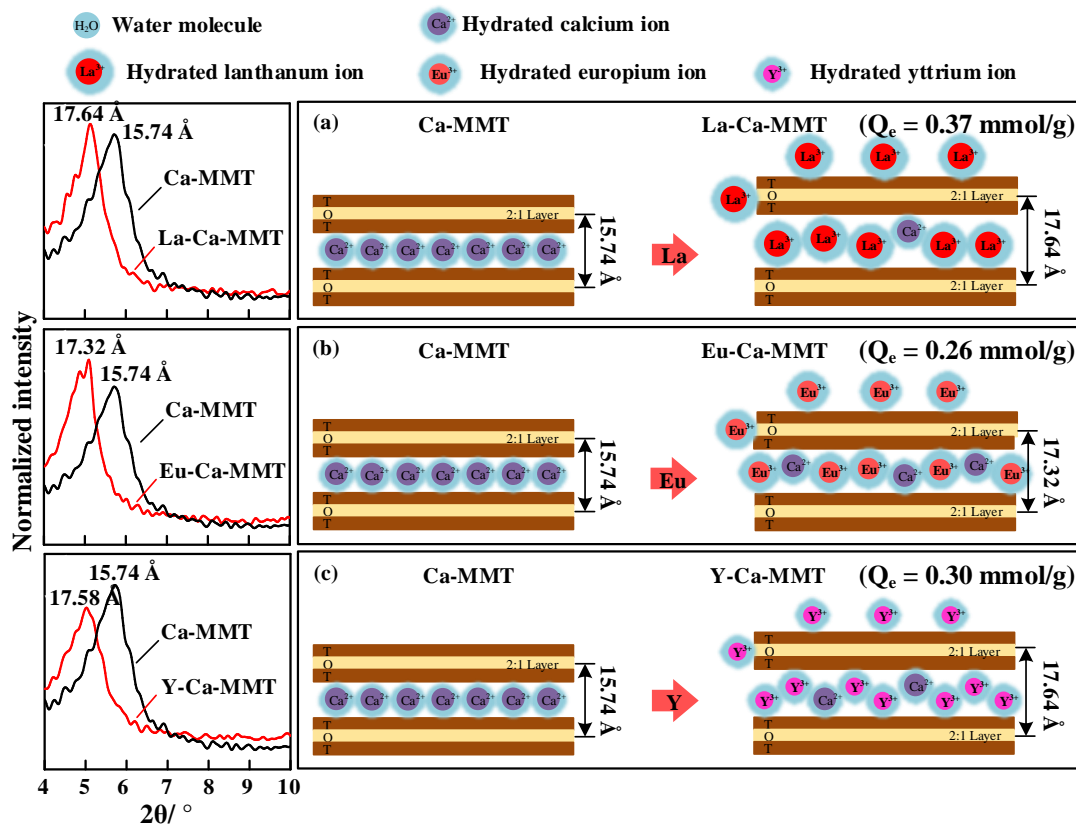


Fig. 4. XRD patterns (left) and assumed schematic diagrams (right) of Ca-MMT before and after La<sup>3+</sup> (a), Eu<sup>3+</sup> (b) or Y<sup>3+</sup> (c) adsorption

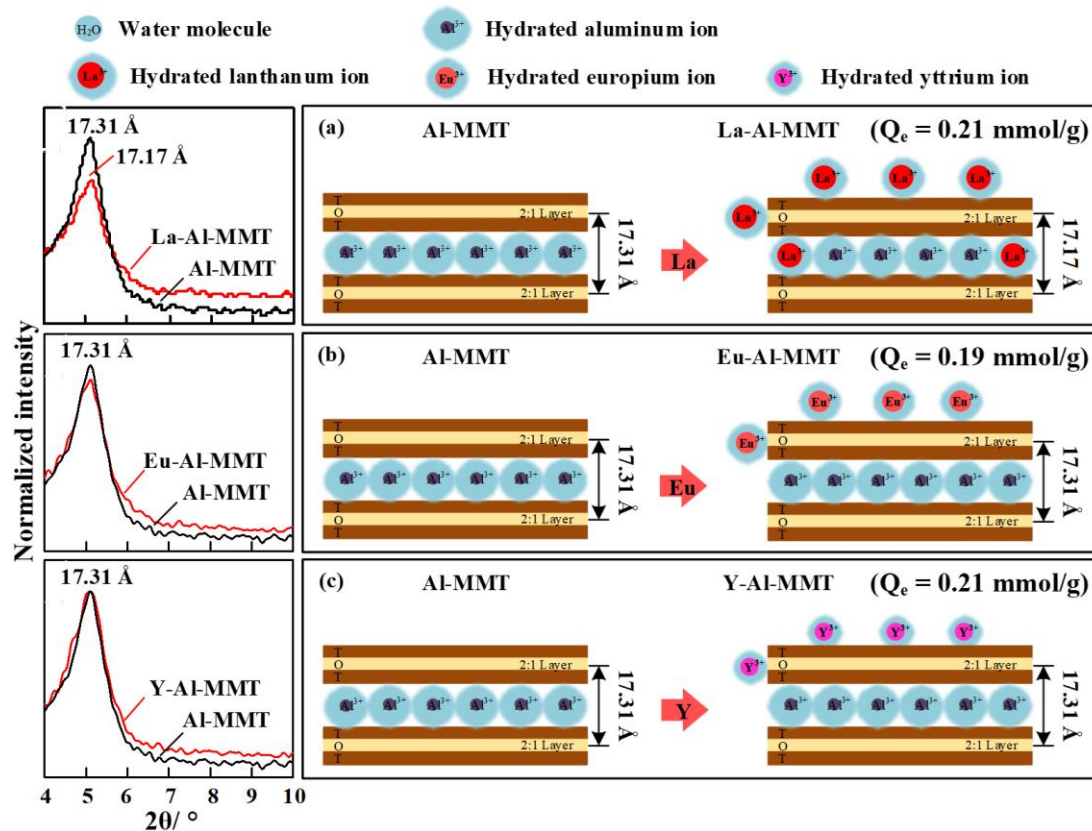


Fig. 5. XRD patterns (left) and assumed schematic diagrams (right) of Al-MMT before and after  $\text{La}^{3+}$  (a),  $\text{Eu}^{3+}$  (b) or  $\text{Y}^{3+}$  (c) adsorption

Ca-MMT. This may be attributed that  $\text{K}^+$ -collapsed interlayer spacing ( $13.22 \text{ \AA}$ ) is than  $\text{Ca}^{2+}$ -collapsed interlayer spacing ( $15.74 \text{ \AA}$ ). It is difficult for the hydrous  $\text{RE}^{3+}$  to intercalate into the  $\text{K}^+$ -collapsed interlayers and exchange with  $\text{K}^+$ . In addition, the hydrous  $\text{RE}^{3+}$  has a high substitution degree with the hydrous  $\text{Ca}^{2+}$  rather than the anhydrous  $\text{K}^+$  in interlayers. The above conclusions about the adsorption capacity are consistent with the results of Table 2.

It can be considered that the saturated adsorption capacity of  $\text{RE}^{3+}$  on the external sites of pretreated MMT is a definite value ( $0.21 \text{ mmol/g}$  for  $\text{La}^{3+}$ ,  $0.19 \text{ mmol/g}$  for  $\text{Eu}^{3+}$  and  $0.21 \text{ mmol/g}$  for  $\text{Y}^{3+}$ ), and the increased adsorption amounts on K-MMT and Ca-MMT are caused by the interlayer adsorption. Therefore, the adsorption capacity of  $\text{RE}^{3+}$  on the interlayer sites of pre-treated MMT follows the order: Ca-MMT ( $\text{La}^{3+}$  ( $0.16 \text{ mmol/g}$ ),  $\text{Y}^{3+}$  ( $0.09 \text{ mmol/g}$ ),  $\text{Eu}^{3+}$  ( $0.07 \text{ mmol/g}$ )) > K-MMT ( $\text{La}^{3+}$  ( $0.09 \text{ mmol/g}$ ),  $\text{Y}^{3+}$  ( $0.07 \text{ mmol/g}$ ),  $\text{Eu}^{3+}$  ( $0.06 \text{ mmol/g}$ )) > Al-MMT (nearly  $0 \text{ mmol/g}$ ). The assumed schematic diagrams of pre-treated MMT before and after  $\text{RE}^{3+}$  adsorption is presented on the right of Fig. 3 to 5.

### 3.3. RE exchangeability in the different binding sites of MMT

The distributions of RE adsorbed on external and interlayer sites have been qualitatively analyzed in the above RE adsorption experiments of the three pretreated MMT. Through the subsequent desorption experiments, the reversibility of RE in different adsorption sites was studied, and an effective cation exchanger for RE removal from these high-affinity sites was also identified. Due to the different ion properties (cations and anion) and effects on desorption, distinct desorption patterns can be expected.  $\text{NH}_4\text{Cl}$ ,  $(\text{NH}_4)_2\text{SO}_4$ ,  $\text{MgCl}_2$  and  $\text{MgSO}_4$  were used to desorb RE from RE-K-MMT, RE-Ca-MMT and RE-Al-MMT by a semi-continuous desorption method and the results are presented in Fig. 6.

It is shown that the summed desorption rate is improved with the increase of desorption numbers. The desorption of RE from the accessible sites is a reversible reaction. Due to the resorption of desorbed RE, the adsorbed RE cannot be completely desorbed by a single desorption (Rigol et al.,

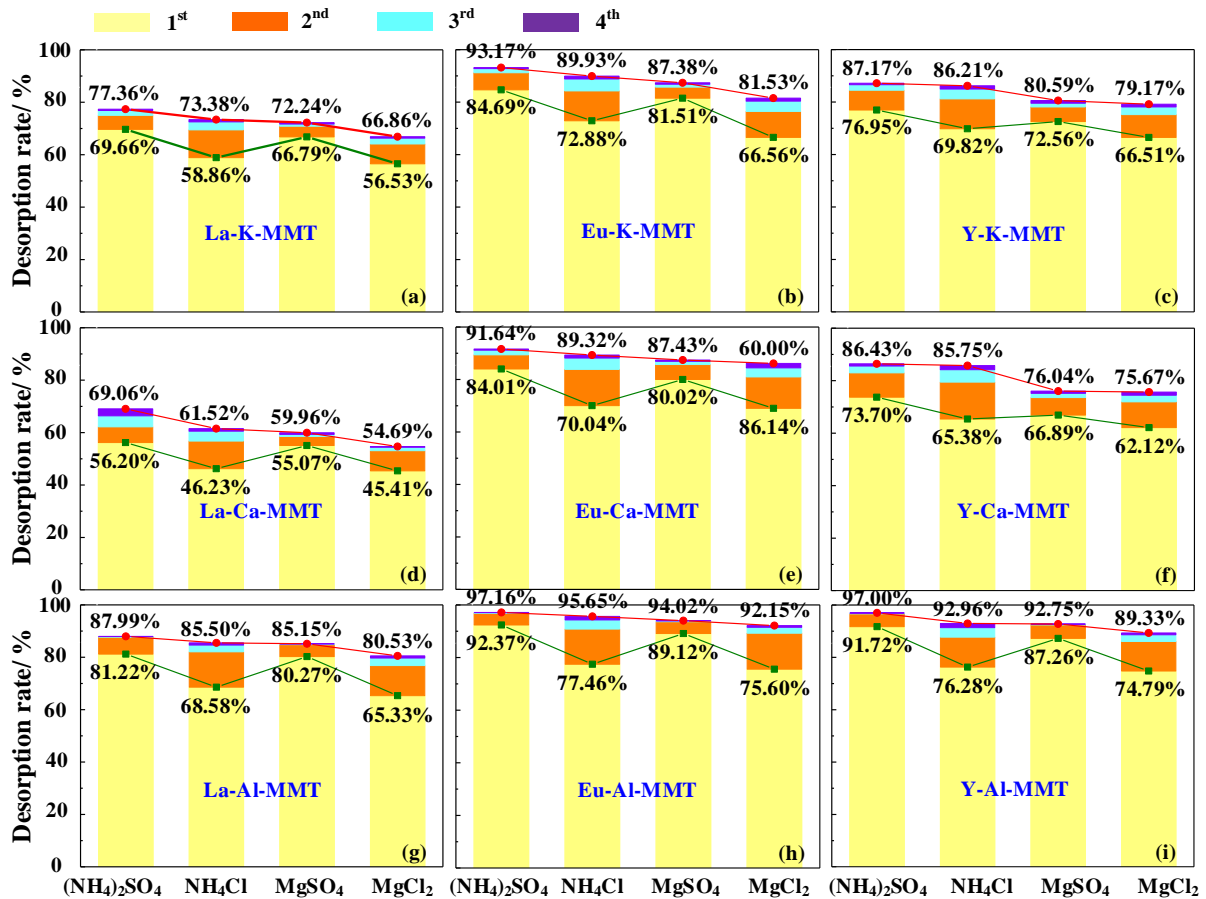


Fig. 6. Semi-continuous desorption of La<sup>3+</sup> (a, d, g), Eu<sup>3+</sup> (b, e, h), Y<sup>3+</sup> (c, f, i) from RE-K-MMT (a, b, c), RE-Ca-MMT (d, e, f) and RE-Al-MMT (g, h, i) with (NH<sub>4</sub>)<sub>2</sub>SO<sub>4</sub>, NH<sub>4</sub>Cl, MgSO<sub>4</sub> and MgCl<sub>2</sub>

1999). This is why the semi-continuous desorption method was used in this study. It is also beneficial to distinguish the effects of interlayer changes on RE desorption. Due to the limited efficiency of a single desorption, the desorbed RE in the first round of desorption can be considered from the external site of the pretreated MMT.

No matter which desorption agents are used, the desorption ratios of RE from RE-Al-MMT in the first round of desorption are highest among the three pretreated MMT. RE adsorbed on Al-MMT is more easily desorbed. It further indicates that RE is adsorbed on the external sites of Al-MMT, nearly not the interlayer sites, and the desorption of ions from the external sites is easier than the interlayer sites. The higher the adsorption amount of RE on the interlayers sites, the more difficult its desorption and the lower the desorption rate of RE. So, even after four rounds of the semi-continuous desorption, the desorption rate of RE is still in the order of RE-Al-MMT > RE-K-MMT > RE-Ca-MMT and Eu<sup>3+</sup> > Y<sup>3+</sup> > La<sup>3+</sup>. These results are consistent with the adsorption amounts of RE on the interlayer sites of the three pretreated MMT. It also suggests that the effect of impurity ions on the exchangeability of RE from MMT is in the order of Ca<sup>2+</sup> > K<sup>+</sup> > Al<sup>3+</sup>.

From the first round of desorption, it is easy to conclude that the desorption ability of the desorption agents for RE adsorbed on the external sites decrease with the order of (NH<sub>4</sub>)<sub>2</sub>SO<sub>4</sub>, MgSO<sub>4</sub>, NH<sub>4</sub>Cl and MgCl<sub>2</sub>. That is to say, the desorption ability of NH<sub>4</sub><sup>+</sup> is larger than Mg<sup>2+</sup> with the same anion, while the desorption ability of SO<sub>4</sub><sup>2-</sup> is larger than Cl<sup>-</sup> with the same cation. In aqueous solution, ions exist in the form of hydration, and their adsorption capacity is determined by the ionic potential or charge density (Xu et al., 2019). When the hydrated cation reaches the absorption sites of RE<sup>3+</sup>, NH<sub>4</sub><sup>+</sup> with low hydration energy can be completely dehydrated and adsorb on the surface of clay minerals to form strong electrostatic bonds, but Mg<sup>2+</sup> with high hydration energy still retains some bound water and adsorb on the surface of clay minerals to form weak electrostatic bonds<sup>[91]</sup> (Moldoveanu and Papangelakis, 1999). Thus, the exchangeability of NH<sub>4</sub><sup>+</sup> with RE<sup>3+</sup> is stronger than

Mg<sup>2+</sup>. Compared with Cl<sup>-</sup>, the hydrated SO<sub>4</sub><sup>2-</sup> with a higher ionic potential is easier to combine with the exposed positive charge on the surface of clay minerals. It increases the electronegativity of clay minerals. And more cations will be attracted into the stern layer of diffusion double electric layers of clay minerals, resulting in the desorption ratio of RE improved (Xu et al., 2019). SO<sub>4</sub><sup>2-</sup> is beneficial for RE desorbing from external sites.

After four rounds of desorption, the total desorption rate of RE decreases with the order of (NH<sub>4</sub>)<sub>2</sub>SO<sub>4</sub>, NH<sub>4</sub>Cl, MgSO<sub>4</sub> and MgCl<sub>2</sub>, which is a little different from that after only one round of desorption. It indicates that anions dominate the desorption of RE from the external sites of clay minerals, while cations dominate the desorption of RE from the interlayer sites of clay minerals. In the first round of desorption, the desorption ability of the desorption agent containing SO<sub>4</sub><sup>2-</sup> is better than that containing Cl<sup>-</sup> due to the RE desorbed almost from the external sites, but with the increasing desorption rounds, the desorption ability of the desorption agent containing NH<sub>4</sub><sup>+</sup> is greater than that contained Mg<sup>2+</sup> due to the RE desorbed from the interlayer sites. Hence, the desorption ability of the desorption agents for RE adsorbed on the interlayer sites decreases with the order of (NH<sub>4</sub>)<sub>2</sub>SO<sub>4</sub>, NH<sub>4</sub>Cl, MgSO<sub>4</sub> and MgCl<sub>2</sub>.

### 3.4. Cationic exchange pathways of RE desorption from different binding sites

In order to clarify the cation exchange mechanism in different binding sites of MMT during the RE desorption process, the XRD patterns of RE-Ca/K/Al-MMT before and after RE desorption with (NH<sub>4</sub>)<sub>2</sub>SO<sub>4</sub>, NH<sub>4</sub>Cl, MgSO<sub>4</sub> and MgCl<sub>2</sub> were compared and the results are shown in Fig. 7. All the basal spacings of RE-Ca/K/Al-MMT change after desorption, indicating that NH<sub>4</sub><sup>+</sup> and Mg<sup>2+</sup> indeed enter the interlayer of RE-Ca/K/Al-MMT and exchange with the RE<sup>3+</sup>, Ca<sup>2+</sup>, K<sup>+</sup> or Al<sup>3+</sup> in the interlayer. The ion exchange in the interlayer is usually more difficult than the external and requires a stronger driving force for the diffusion of desorption cations into the interlayer. In order to desorb more RE ions and obtain a high desorption rate, multiple desorptions are required. In every round of desorption, the fresh desorption solution will provide a large diffusion driving force for NH<sub>4</sub><sup>+</sup> or Mg<sup>2+</sup> to arrive at the exchange sites in the interlayer. And the difficulty for desorption cations reaching the exchange sites increases from the edge side to the core of the interlayer. So, as the increasing rounds of desorption, the desorption rate increases but the increase of the desorption rate reduces.

The anhydrous NH<sub>4</sub><sup>+</sup> with a small ion radius replaces the hydrated RE<sup>3+</sup>, Ca<sup>2+</sup> or Al<sup>3+</sup> with a large ion radius in the interlayer, which causes the interlayer collapse and the change of the basal spacings ( $\Delta d > 2.64 \text{ \AA}$ ) great. While the change of the basal spacings ( $\Delta d < 0.52 \text{ \AA}$ ) is slight using magnesium salt as a desorption agent due to the hydrated ion radius of Mg<sup>2+</sup> (4.28 Å) close to the original interlayer cations. According to the results published by Pestana et al. (2017), the change of the basal spacings ( $\Delta d$ ) can reflect the activation energy barriers ( $\Delta E$ ) for ion migration within interlayers to some extent, and  $\Delta E$  decreases linearly with the increase of  $\Delta d$ . Compared to Mg<sup>2+</sup>, the larger  $\Delta d$  may provide a smaller  $\Delta E$  for NH<sub>4</sub><sup>+</sup> diffusion within interlayers. In other words, NH<sub>4</sub><sup>+</sup> is easier to enter the interlayer, even diffuse from the edge side to the core of the interlayer, and exchange more cations (Pestana et al., 2017). Thus, the desorption capacity of NH<sub>4</sub><sup>+</sup> for the interlayer ions is better, and the desorption rate of RE with ammonium salt is higher than with magnesium salt.

As described in part 3.2, mostly all RE<sup>3+</sup> adsorb on the external sites of Al-MMT. Nevertheless, the basal spacing of RE-Al-MMT is altered after desorption, implying that Al<sup>3+</sup> in the interlayer is exchanged by NH<sub>4</sub><sup>+</sup> or Mg<sup>2+</sup>. Due to the high desorption capacity of NH<sub>4</sub><sup>+</sup> for the interlayer ions, the amount of Al<sup>3+</sup> desorbed by NH<sub>4</sub><sup>+</sup> must be more than Mg<sup>2+</sup>. It causes the concentration of impurity ions in the solution to be higher using ammonium salt as the desorption agent compared to magnesium salt. The obtained results are well consistent with the published results (Xiao et al., 2015a).

### 3.5. Implications for RE migration in RE ores and its recovery

In natural surroundings, the decomposition of organic matter and the partial dissolution of minerals in acidic environments cause the various cations (e.g., K<sup>+</sup>, NH<sub>4</sub><sup>+</sup>, Ca<sup>2+</sup>, Mg<sup>2+</sup> and Al<sup>3+</sup>) to be released into the soil (Dzene et al., 2017). In the RE ore, these released cations will migrate down with the migration of rainwater and partially adsorb on the clay minerals. Some cations are adsorbed on the external sites of clay minerals, while others exchange with the interlayer cations and modify the struc-

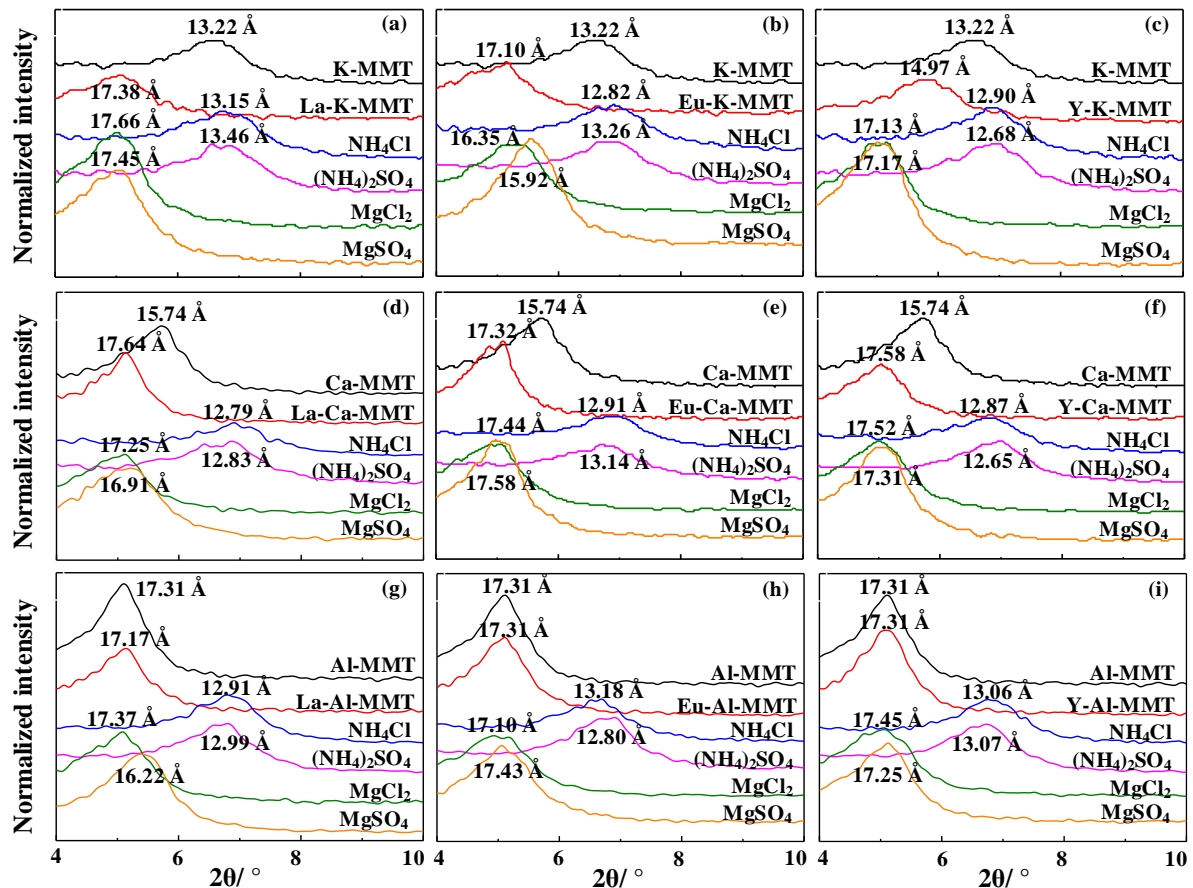


Fig. 7. XRD patterns of RE-K-MMT (a, b, c), RE-Ca-MMT (d, e, f) and RE-Al-MMT (g, h, i) before and after the desorption of  $\text{La}^{3+}$  (a, d, g),  $\text{Eu}^{3+}$  (b, e, h) and  $\text{Y}^{3+}$  (c, f, i) with  $(\text{NH}_4)_2\text{SO}_4$ ,  $\text{NH}_4\text{Cl}$ ,  $\text{MgCl}_2$  and  $\text{MgSO}_4$

ture of the clay minerals. It will affect the adsorption of  $\text{RE}^{3+}$  at different sites and further impact the migration behaviors of RE in the orebody. The adsorption of cations with low hydration energy and small hydration radius in the interlayers leads to the collapse of the interlayer so that the resistance of  $\text{RE}^{3+}$  entering the interlayer increases, and the adsorption amount of RE in the interlayer decreases. In this study, the adsorption of  $\text{K}^+$  and  $\text{Ca}^{2+}$  in the interlayer of MMT leads to the collapse of the interlayer. And the degree of interlayer collapse by  $\text{K}^+$  ( $d_{001}=13.22 \text{ \AA}$ ) is more severe than  $\text{Ca}^{2+}$  ( $d_{001}=15.74 \text{ \AA}$ ) due to a smaller ion radius and hydration energy. The adsorption amount of RE in the interlayer of K-MMT is smaller than Ca-MMT. MMT pre-saturated with  $\text{Al}^{3+}$  was acidic, which was not conducive to the adsorption of  $\text{RE}^{3+}$ . The RE minerals in the protolith (e.g., gadolinite, bastnaesite, aeschynite) are weathered and dissociated to hydrated RE ions or hydroxyl hydrated RE ions. These RE ions migrate down with the migration of rainwater and partially adsorb on the clay minerals. Then the weathered crust elution-deposited RE ore is formed, in which RE mainly exists as the exchangeable state. From the above results about the effects of  $\text{K}^+$ ,  $\text{Ca}^{2+}$  and  $\text{Al}^{3+}$  on the RE adsorption in binding sites of clay minerals, it can be predicted that the grade of the exchangeable RE in the ore abundant in  $\text{Ca}^{2+}$  is the most, followed by the ore rich in  $\text{K}^+$  and  $\text{Al}^{3+}$  the least.

The adsorption of RE in interlayers, especially in collapsed interlayers, has a significant influence on the reversibility of RE. According to the semi-continuous desorption experiments with  $\text{NH}_4\text{Cl}$ ,  $(\text{NH}_4)_2\text{SO}_4$ ,  $\text{MgCl}_2$  and  $\text{MgSO}_4$ , it can be found that the reversibility of RE adsorbed in interlayers, especially in collapsed interlayers, is far worse than the one adsorbed on externals. In other words, the desorption of RE in interlayers, especially collapsed interlayers, seems to be rather difficult. Monovalent  $\text{NH}_4^+$  with a small ionic radius ( $1.48 \text{ \AA}$ ) and low hydration energy ( $322 \text{ kJ/mol}$ ) may readily arrive at frayed edge sites (FES) and exchange  $\text{RE}^{3+}$ . By contrast, divalent  $\text{Mg}^{2+}$  with a large hydrated radius ( $4.28 \text{ \AA}$ ) and high hydration energy ( $1828 \text{ kJ/mol}$ ) may have difficulty entering the wedge zone of FES (Coleman et al., 1963; Sawhney, 1972), so they are generally thought to desorb RE

mostly from accessible external sites. The ion exchange capacity of  $\text{NH}_4^+$  with  $\text{RE}^{3+}$  is stronger than that of  $\text{Mg}^{2+}$ , especially with  $\text{RE}^{3+}$  in collapsed interlayers. Therefore, the recovery rate of RE from WCED-REO with ammonium salts is better than that with magnesium salts.

From the published results (Chen et al., 2018; He et al., 2016; Xiao et al., 2015b), it can be noted that with the increasing concentration of  $\text{NH}_4^+$  and  $\text{Mg}^{2+}$ , not only the recovery rate of RE from WCED-REO are improved, but also the kinetic and mass transfer process is enhanced. A high concentration gradient of  $\text{NH}_4^+$  or  $\text{Mg}^{2+}$  can promote its diffusion from solution to the surface of particles, then to the interior and exchange more  $\text{RE}^{3+}$ . In the solution, the ionic radius of  $\text{NH}_4^+$  is smaller than the hydrated radius of  $\text{RE}^{3+}$ , so the ion exchange between  $\text{NH}_4^+$  and  $\text{RE}^{3+}$  must lead to the interlayer collapse. The interlayer collapse will hinder the diffusion of  $\text{NH}_4^+$  from the edge of the interlayer to the core. But it can be overcome by a driving force provided by a high concentration gradient of  $\text{NH}_4^+$ . In the desorption of interlayer  $\text{RE}^{3+}$  with  $\text{NH}_4^+$ , the enhancing effect of interlayer diffusion plays a dominant role, not the hindering effect of interlayer collapse. Unlike  $\text{NH}_4^+$ , the hydrated radius of  $\text{Mg}^{2+}$  is approach to that of  $\text{RE}^{3+}$ . The change of the basal spacings is slight after the desorption of interlayer  $\text{RE}^{3+}$  with  $\text{Mg}^{2+}$ . There is almost no hindering effect of interlayer collapse, but the large hydrated radius may limit the migration of  $\text{Mg}^{2+}$  in the interlayer. It causes that the desorption capacity of  $\text{Mg}^{2+}$  for interlayer  $\text{RE}^{3+}$  is worse than that of  $\text{NH}_4^+$ . The migration of  $\text{Mg}^{2+}$  in the interlayer also can be enhanced by providing a high and persistent concentration gradient.  $\text{Mg}^{2+}$  first desorb  $\text{RE}^{3+}$  from external sites, then replace  $\text{RE}^{3+}$  in FES or interlayer sites near the edge side and eventually exchange  $\text{RE}^{3+}$  from the core of interlayer. But the complete desorption of  $\text{RE}^{3+}$  by  $\text{Mg}^{2+}$  may be a kinetic-controlled process involving the cation migration in interlayers and may take days, months or even years.

#### 4. Conclusions

In this study, the effects of  $\text{K}^+$ ,  $\text{Ca}^{2+}$  and  $\text{Al}^{3+}$  on  $\text{RE}^{3+}$  adsorption and desorption in binding sites of MMT were investigated. Through the pre-saturation, the interlayer ions of MMT had been replaced by  $\text{K}^+$ ,  $\text{Ca}^{2+}$  or  $\text{Al}^{3+}$ . The adsorption of  $\text{K}^+$  and  $\text{Ca}^{2+}$  leads to the interlayer collapse of MMT and the collapse degree of interlayer by  $\text{K}^+$  is larger than  $\text{Ca}^{2+}$  due to a smaller ion radius of  $\text{K}^+$ . Ca-MMT provides a smaller hinder effect of interlayer collapse for the interlayer diffusion of  $\text{RE}^{3+}$ , results in its adsorption capacity for RE is larger than K-MMT. MMT pre-saturated with  $\text{Al}^{3+}$  was acidic, which was not conducive to the adsorption of  $\text{RE}^{3+}$ . It can be predicted that the grade of the exchangeable RE in WCED-REO abundant in  $\text{Ca}^{2+}$  is the most, followed by the ore rich in  $\text{K}^+$  and  $\text{Al}^{3+}$  the least.

The exchangeability of RE was studied with  $\text{NH}_4\text{Cl}$ ,  $(\text{NH}_4)_2\text{SO}_4$ ,  $\text{MgCl}_2$  and  $\text{MgSO}_4$  by a semi-continuous desorption method. The results showed that the reversibility of RE adsorbed in interlayers, especially in collapsed interlayers, is far worse than the one adsorbed on externals. The desorption rates of RE were in the order of RE-Al-MMT > RE-K-MMT > RE-Ca-MMT. Compared with  $\text{Mg}^{2+}$ ,  $\text{NH}_4^+$  with a smaller ionic radius and low hydration energy may easier to arrive FES and exchange  $\text{RE}^{3+}$ . The ion exchange capacity of  $\text{NH}_4^+$  with  $\text{RE}^{3+}$  is stronger than that of  $\text{Mg}^{2+}$ , especially  $\text{RE}^{3+}$  in collapsed interlayers. Therefore, the recovery rate of RE from WCED-REO with ammonium salts is better than that with magnesium salts. The results can enrich the metallogeny theory of WCE-DREO and provide a certain theoretical basis for its efficient exploitation.

#### Acknowledgments

The work is financially supported by grants from the National Natural Science Foundation of China (U2002215) and "the Fundamental Research Funds for the Central Universities", South-Central University for Nationalities (CZQ22001, CZQ23034).

#### References

- ALSHAMERI, A., HE, H.P., XIN, C., ZHU, J.X., WEI, X.H., ZHU, R.L., WANG, H.L., 2019. *Understanding the role of natural clay minerals as effective adsorbents and alternative source of rare earth elements: Adsorption operative parameters*. Hydrometallurgy 185, 149-161.
- BENEDICTO, A., MISSANA, T., FERNÁNDEZ, A.M., 2014. *Interlayer collapse affects on cesium adsorption onto illite*.

- Environ. Sci. Technol. 48(9), 4909-4915.
- CHEN, Z., ZHANG, Z.Y., HE, Z.Y., CHI, R.A., 2018. *Mass transfer process of leaching weathered crust elution-deposited rare earth ore with magnesium salts*. Physicochem. Probl. Miner. Process. 54(3), 1004-1013.
- CHEN, Z.H., 2011. *Global rare earth resources and scenarios of future rare earth industry*. J. Rare Earth 29(1), 1-6.
- CHI, R.A., TIAN, J., 2008. *Weathered crust elution-deposited rare earth ores*. New York: Nova Science Publishers.
- CHI, R.A., TIAN, J., LI Z.J., PENG, C., WU Y.X., LI S.R., WANG, C.W., ZHOU Z.A., 2005. *Existing state and partitioning of rare earth on weathered ores*. J. Rare Earth 23(6), 756-759.
- CHI, R.A., WANG, D.Z., 2014. *Rare earth mineral processing*. Beijing: Science Press.
- COLEMAN, N.T., LEWIS, R.J., CRAIG, D., 1963. *Sorption of cesium by soils and its displacement by salt solutions*. Soil Sci. Soc. Am. J. 27, 290-294.
- COPPIN, F., BERGER, G., BAUER, A., CASTET, S., LOUBET, M., 2002. *Sorption of lanthanides on smectite and kaolinite*. Chem. Geol. 182, 57-68.
- DZENE, L., FERRAGE, E., VIENNET, J.C., TERTRE, E., HUBERT, F., 2017. *Crystal structure control of aluminized clay minerals on the mobility of caesium in contaminated soil environments*. Sci. Rep-UK. 7(1), 1-12.
- DZENE, L., TERTRE, E., HUBERT, F., FERRAGE, E., 2015. *Nature of the sites involved in the process of cesium desorption from vermiculite*. J. Colloid Interf. Sci. 455, 254-260.
- FAN, Q.H., TANAKA, M., TANAKA, K., SAKAGUCHI, A., TAKAHASHI, Y., 2014. *An EXAFS study on the effects of natural organic matter and the expandability of clay minerals on cesium adsorption and mobility*. Geochim. Cosmochim. Ac. 135, 49-65.
- FENG, J., YU, J.X., HUANG, S.X., WU, X.Y., ZHOU, F., XIAO, C.Q., XU, Y.L., CHI, R.A., 2021. *Effect of potassium chloride on leaching process of residual ammonium from weathered crust elution-deposited rare earth ore tailings*. Miner. Eng. 163, 1-8.
- HE, Z.Y., ZHANG, Z.Y., YU, J.X., XU, Z.G., XU, Y.L., ZHOU, F., CHI, R.A., 2016. *Column leaching process of rare earth and aluminum from weathered crust elution-deposited rare earth ore with ammonium salts*. T. Nonferr. Metal Soc. 26, 3024-3033.
- HUANG, S.X., FENG, J., YU, J.X., WANG, Y., LIU, J.Q., CHI, R.A., HOU, H.B., 2021. *Adsorption and desorption performances of ammonium on the weathered crust elution-deposited rare earth ore*. Colloid Surface A. 613, 126-139.
- KANAZAWA, Y., KAMITANI, M., 2006. *Rare earth minerals and resources in the world*. J. Alloy Compd. 408, 1339-1343.
- KRISHNA, G.B., SUSMITA, S.G., 2009. *Calcined tetrabutylammonium kaolinite and montmorillonite and adsorption of Fe(II), Co(II) and Ni(II) from solution*. Appl. Clay Sci. 46(2), 216-221.
- LEE, J., PARK, S.M., JEON, E.K., BAEK, K., 2017. *Selective and irreversible adsorption mechanism of cesium on illite*. Appl. Geochem. 85, 188-193.
- LI, Y.X., 2014. *Ion adsorption type rare earth resources and green extraction*. Beijing: Chemical Industry Press.
- MARCUS Y., 1985. *Ion solvation*. New York: John Wiley & Sons Ltd., USA.
- MOLDOVEANU, G.A., PAPANGELAKIS, V.G., 2012. *Recovery of rare earth elements adsorbed on clay minerals: I. Desorption mechanism*. Hydrometallurgy. 117-118, 71-78.
- PESTANA, L.R., KOLLURI, K., HEAD-GORDON, T., LAMMERS, L.N., 2017. *Direct exchange mechanism for interlayer ions in non-swelling clays*. Environ. Sci. Technol. 51, 393-400.
- POPE, C.G., 1997. *X-ray diffraction and the Bragg equation*. J. Chem. Educ. 74, 129-131.
- RIGOL, A., VIDAL, M., RAURET, G., 1999. *Effect of the ionic status and drying on radiocesium adsorption and desorption in organic soils*. Environ. Sci. Technol. 33, 3788-3794.
- SAWHNEY, B. L., 1972. *Selective sorption and fixation of cations by clay minerals: A review*. Clays Clay Miner. 20, 93-100.
- SINITSYN, V.A., AJA, S.U., KULIK, D.A., WOOD, S.A., 2000. *Acid-base surface chemistry and sorption of some lanthanides on K<sup>+</sup>-saturated Marblehead illite: I. Results of an experimental investigation*. Geochim. Cosmochim. Ac. 64, 185-194.
- TANSEL, B., 2012. *Significance of thermodynamic and physical characteristics on permeation of ions during membrane separation: Hydrated radius, hydration free energy and viscous effects*. Sep. Purif. Technol. 86, 119-126.
- TANSEL, B., SAGER, J., RECTOR, T., GARLAND, J., STRAYER, R.F., LEVINE, L., ROBERTS, M., HUMMERICK, M., BAUER, J., 2006. *Significance of hydrated radius and hydration shells on ionic permeability during nanofiltration in dead end and cross flow modes*. Sep. Purif. Technol. 51(1), 40-47.

- TERTRE, E.; FERRAGE, E.; BIHANNIC, I.; MICHOT, L.J.; PRÊT, D., 2011. *Influence of the ionic strength and solid/solution ratio on Ca(II)-for-Na<sup>+</sup> exchange on montmorillonite. Part 2: Understanding the effect of the m/V ratio. Implications for pore water composition and element transport in natural media.* J. Colloid Interf. Sci. 363(1), 334-347.
- TIAN, J., TANG, X.K., YIN, J.Q., LUO, X.P., RAO, G.H., JIANG, M.T., 2013. *Process optimization on leaching of a lean weathered crust elution-deposited rare earth ores.* Int. J. Miner. Process. 119, 83-88.
- TOMBACZ, E., SZEKERES, M., 2004. *Colloidal behavior of aqueous montmorillonite suspensions: the specific role of pH in the presence of indifferent electrolytes.* Appl. Clay Sci. 27(1-2), 75-94.
- WAN, Y.X., LIU, C.Q., 2006. *The effect of humic acid on the adsorption of REEs on kaolin.* Colloid Surface A. 290(1-3), 112-117.
- XIAO, Y.F., CHEN, Y.Y., FENG, Z.Y., HUANG, X.W., HUANG, L., LONG, Z.Q., CUI, D.L., 2015a. *Leaching characteristics of ion-adsorption type rare earths ore with magnesium sulfate.* T. Nonferr. Metal Soc. 25(11), 3784-3790.
- XIAO, Y.F., FENG, Z.Y., HU, G.H., HUANG, L., HUANG, X.W., CHEN, Y.Y., ZHIQI, LONG, Z.Q., 2016a. *Reduction leaching of rare earth from ion-adsorption type rare earths ore with ferrous sulfate.* J. Rare Earth 34(9), 917-923.
- XIAO, Y.F., FENG, Z.Y., HUANG, X.W., HUANG, L., CHEN, Y.Y., WANG, L.S., LONG, Z.Q., 2015b. *Recovery of rare earths from weathered crust elution-deposited rare earth ore without ammonia-nitrogen pollution: I. leaching with magnesium sulfate.* Hydrometallurgy. 153, 58-65.
- XIAO, Y.F., HUANG, L., LONG, Z.Q., FENG, Z.Y., WANG, L.S., 2016b. *Adsorption ability of rare earth elements on clay minerals and its practical performance.* J. Rare Earth. 34(5), 543-548.
- XIAO, Y.F., LAI, F.G., HUANG, L., FENG, Z.Y., LONG, Z.Q., 2017. *Reduction leaching of rare earth from ion-adsorption type rare earths ore: II. Compound leaching.* Hydrometallurgy 173, 1-8.
- XIAO, Y.F., LIU, X.S., FENG, Z.Y., HUANG, X.W., HUANG, L., CHEN, Y.Y., WU, W.Y., 2015c. *Role of minerals properties on leaching process of weathered crust elution-deposited rare earth ore.* J. Rare Earth. 33(5), 545-552.
- XU, Q.H., SUN, Y.Y., YANG, L.F., LI, C.C., ZHOU, X.Z., CHEN, W.F., LI, Y.X., 2019. *Leaching mechanism of ion-adsorption rare earth by mono valence cation electrolytes and the corresponding environmental impact.* J. Clean. Prod. 211, 566-573.
- YANG, L.F., LI, C.C., WANG, D.S., LI, F.Y., LIU, Y.Z., ZHOU, X.Z., LIU, M.B., WANG, X.F., LI, Y.X., 2019. *Leaching ion adsorption rare earth by aluminum sulfate for increasing efficiency and lowering the environmental impact.* J. Rare Earth. 37(4), 429-436.
- YANG, M.J., LIANG, X.L., MA, L.Y., HUANG, J., HE, H.P., ZHU, J.X., 2019. *Adsorption of REEs on kaolinite and halloysite: A link to the REE distribution on clays in the weathering crust of granite.* Chem. Geol. 525, 210-217.
- YIN, X.B., WANG, X.P., WU, H., TAKAHASHI, H., INABA, Y., OHNUKI, T., TAKESHITA, K., 2017. *Effects of NH<sub>4</sub><sup>+</sup>, K<sup>+</sup>, Mg<sup>2+</sup>, and Ca<sup>2+</sup> on the cesium adsorption/desorption in binding sites of vermiculitized biotite.* Environ. Sci. Technol. 51, 13886-13894.
- YU, B.Z., HU, Z.Y., ZHOU, F., FENG, J., CHI, R.A., 2019. *Lanthanum (III) and yttrium (III) adsorption on montmorillonite: The role of aluminum ion in solution and minerals.* Miner. Process. Ext. Met. Rev. 41(2), 1-10.
- ZHAO, X.Y., ZHANG, Y.Y., 1990. *Analysis of clay minerals and clay minerals.* Beijing: Ocean Press.
- ZHOU, F., FENG, J., XIE, X., WU, B.H., LIU, Q., WU, X.Y., CHI, R.A., 2019. *Adsorption of lanthanum (III) and yttrium (III) on kaolinite: kinetics and adsorption isotherms.* Physicochem. Probl. Mi. 55(4), 928-939.